

Mutated *nup62* Causes Autosomal Recessive Infantile Bilateral Striatal Necrosis

Lina Basel-Vanagaite, MD, PhD,^{1,2} Liora Muncher, MSc,² Rachel Straussberg, MD,^{2,3} Metsada Pasmanik-Chor, PhD,⁴ Michal Yahav, PhD,² Limor Rainshtein, MSc,⁵ Christopher A. Walsh, MD, PhD,^{6,7} Nurit Magal, PhD,^{2,5} Ellen Taub, MSc,¹ Valerie Drasinover, MSc,⁵ Hanna Shalev, MD,⁸ Revital Attia, MSc,⁵ Gideon Rechavi, MD, PhD,^{2,9} Amos J. Simon, PhD,^{2,9} and Mordechai Shohat MD^{1,2}

Objective: The objective of this study was to identify the gene causing autosomal recessive infantile bilateral striatal necrosis.

Methods: We have mapped the disease gene in the candidate region to approximately 230kb on 19q13.33 in 8 interrelated families including a total of 12 patients and 39 unaffected individuals.

Results: Sequencing of the *nup62* gene showed a missense mutation causing a change from glutamine to proline (Q391P) in all the patients, producing a substitution from a polar, hydrophilic residue to a nonpolar, neutral residue. All the other 12 candidate genes were sequenced, and no pathogenic sequence changes were found. Comparisons of p62 protein sequences from diverse species indicate that glutamine at position 391 is highly conserved. Five prenatal diagnoses were performed in three at-risk families.

Interpretation: This is the second example of a nuclear pore complex protein causing mendelian disease in humans (the first one is triple A syndrome). Our findings suggest that p62 has a cell type-specific role and is important in the degeneration of the basal ganglia in humans.

Ann Neurol 2006;60:214–222

Infantile bilateral striatal necrosis (IBSN; MIM 271930) is a neurological disorder characterized by symmetrical degeneration of the caudate nucleus, putamen, and occasionally the globus pallidus, with little involvement of the rest of the brain.¹ The clinical features of IBSN include developmental regression, choreoathetosis, dystonia, spasticity, dysphagia, failure to thrive, nystagmus, optic atrophy, and mental retardation.² Familial IBSN has been reported.^{3–9} In families with mitochondrial inheritance, mutations in the adenosine triphosphatase 6 gene (complex V) have been described.^{10,11}

We have previously identified and evaluated clinically six consanguineous families with autosomal recessive IBSN.¹² We have mapped the candidate locus for IBSN to the chromosomal region 19q13.32–13.41, between the markers D19S596 and D19S867, spanning a 1.2Mb chromosomal region.¹³ In this study, we have

further reduced the candidate region to 230kb on 19q13.33 between the markers rs8101959 and D19S867 and have identified the disease-causing mutation in all six original families and two additional families.

Subjects and Methods

Subjects

We ascertained a total of 8 Israeli Bedouin families with IBSN with 12 affected and 39 unaffected individuals, including 6 interrelated families who have been described previously^{12,13} and 2 new families identified during this study. All the families bear the same family name. The exact relationships among five of the families are known,¹² whereas those of the three remaining families to the other five families are unknown. Straussberg and colleagues¹² have described the clinical manifestations, radiological evolution, and neuropathological characteristics of the disease in the original fam-

From the ¹Department of Medical Genetics, Schneider Children's Medical Center of Israel and Rabin Medical Center, Petah Tikva; ²Sackler Faculty of Medicine, Tel Aviv University, Tel Aviv; ³Neurogenetic Clinic, Schneider Children's Medical Center of Israel, Petah Tikva; ⁴Bioinformatics Unit, G.S.W. Faculty of Life Sciences, Tel Aviv University, Tel Aviv; ⁵Felsenstein Medical Research Center, Petah Tikva, Israel; ⁶Howard Hughes Medical Institute, Beth Israel Deaconess Medical Center; ⁷Department of Neurology, Harvard Medical School, Boston, MA; ⁸Pediatrics Department, Soroka Medical Center, Beersheba; and ⁹Sheba Cancer Research Center, Institute of Hematology, The Chaim Sheba Medical Center, Ramat-Ban, Israel.

Received Mar 1, 2006, and in revised form Apr 18. Accepted for publication Apr 28, 2006.

L.B.-V. and L.M. contributed equally to this work.

Published online Jun 19, 2006 in Wiley InterScience (www.interscience.wiley.com). DOI: 10.1002/ana.20902

Address correspondence to Dr Basel-Vanagaite, Department of Medical Genetics, Schneider Children's Medical Center of Israel and Rabin Medical Center, Beilinson Campus, Petah Tikva, 49100 Israel. E-mail: basel@post.tau.ac.il

ily. The age of onset of the disease in the affected individuals ranged from 7 to 15 months. The most prominent neurological findings were choreoathetoid movements of the face, trunk and extremities, dystonia, horizontal pendular nystagmus, optic atrophy, and spastic quadriplegia. Gradual disappearance of the basal ganglia was evident on serial brain magnetic resonance imaging (MRI) scans. Initial MRI scans, performed on 3 symptomatic patients at 11, 12, and 15 months, showed no abnormalities. At 20 to 21 months old, MRI scans showed caudate nuclei and putamen of normal size, but on T2-weighted images, bilateral, symmetrical, hyperintense signals were visible in the putamen. Follow-up at 6 years showed further changes. The caudate nucleus and putamen were atrophic, and the putamen showed a low signal on T1-weighted images and a high signal on T2-weighted images. At 10 to 11 years old, MRI scans showed a small, residual caudate nucleus and putamen with abnormal signals. Diffuse parenchymal loss was evident.

Extensive metabolic workup was normal. We obtained informed consent either from all the family members who agreed to participate in the study or from their legal guardians. The research study was reviewed and approved by the Human Subjects Committee of the Rabin Medical Center (Petah Tikva, Israel).

Microsatellite Marker Analysis

DNA was isolated from the blood samples by standard methods.¹⁴ Microsatellite markers were amplified by multiplex polymerase chain reaction (PCR), using standard protocols. Amplified markers were electrophoresed on an ABI 3700 DNA capillary sequencer and were analyzed with GENESCAN and GENOTYPER software (Applied Biosystems, Foster City, CA).

Single Nucleotide Polymorphism Analysis

Sequencing of the single nucleotide polymorphisms was performed with primer sets designed using the Primer 3 program. The genomic sequence was taken from the University of California, Santa Cruz (UCSC) Genome Browser.

Sequencing of Candidate Genes

Sequencing of the candidate genes was performed with primer sets designed using the Primer 3 program. All exons including exon-intron junctions and 5' and 3' untranslated regions were amplified from genomic DNA with primers designed from the genomic sequences available from UCSC Genome Browser. Both strands of the PCR products were sequenced with BigDye Terminators (Applied Biosystems) on an ABI 3100 sequencer. Sequence chromatograms were analyzed using SeqScape software version 1.1 (Applied Biosystems). We initially tested one affected individual, one heterozygous parent, and a noncarrier sibling (as defined by haplotype analysis).

Molecular Analysis of the nup62 Gene

Based on the predicted genomic sequence, 16 primer pairs were used for PCR amplification of exons and exon-intron junctions (primer sequences are available on request). *Nup62* mutation screening was performed on genomic DNA by PCR amplification using the following primers: primer A

(forward): ACGCTGATCGAGAATGGAGA, primer B (reverse): TTTTCTCACGCTCCTCATCC; the PCR product was digested with *Nci*I (New England Biolabs, Beverly, MA). The normal allele produced an uncut fragment of 208bp, and the abnormal allele produced two fragments of 125 and 83 bp.

Western Blot

The lymphoblastoid cell proteins were prepared. Cells were washed twice with phosphate-buffered saline and lysed at 4°C with lysis buffer. After incubation, cell lysates were centrifuged and the supernatants were collected. The pellet fraction was vortexed at 4°C, and the proteins were collected. Proteins from the two fractions were determined using the BCA Protein Assay Reagent Kit (Pierce, Rockford, IL). Whole-cell proteins were subjected to 12% sodium dodecyl sulfate-polyacrylamide gel electrophoresis and transferred to nitrocellulose membranes. The membranes were blocked with 5% skim milk in tris(hydroxymethyl)aminomethane-buffered saline (TBS)-Tween buffer for 30 minutes at room temperature and subsequently incubated with primary monoclonal mouse Mab414 anti-p62 antibodies (1:2,500; Covance Research Products, Berkeley, CA). After washing with TBS-Tween, further incubation for 1 hour with peroxidase-conjugated goat anti-mouse IgG (1:5,000; Jackson ImmunoResearch Laboratories, West Grove, PA) was performed. Immunoreactive proteins were visualized by an ECL (enhanced chemiluminescence super signal) Detection Kit (Pierce). Rabbit polyclonal antibodies to Emerin (Santa Cruz Biotechnology, Santa Cruz, CA) were used to demonstrate equal loading level.

IMMUNOFLUORESCENCE OF LYMPHOBLASTOIDS. Human lymphoblastoid cells were cytospun onto slides. The cells were fixed with ice-cold methanol for 5 minutes and ice-cold acetone for a further 5 minutes, washed with TBS, and blocked using 5% skim milk in TBS containing 0.1% Tween 20 (TBS-T) for 30 minutes. Incubations with primary mouse monoclonal p62 antibodies (1:100; BD Transduction Laboratories, San Jose, CA) and secondary Cy3-conjugated goat anti-mouse antibodies (1:500) were performed in blocking solution for 1 hour each. Between and after the incubation with the antibodies, cells were washed three times with TBS-Tween. The slides were mounted using 46'-diaminidino-2-phenylindole-2 hydrochloride containing Fluoromount-G (Southern Biotechnology, Birmingham, AL), and the cells were photographed using the Improvision (Improvision, Coventry, United Kingdom) optic grid confocal fluorescent microscope (Olympus, Melville, NY).

GENERATION OF YELLOW FLUORESCENT PROTEINS (YFP)-P62 FUSED CONSTRUCTS. RNA was extracted from the patient's and control subject's lymphoblastoid cell lines using RNeasy Mini Kit (Qiagen, Chatsworth, CA) according to the manufacturer's protocol. Complementary DNA (cDNA) was synthesized by RT-PCR using the EZ-First strand cDNA synthesis kit manufactured by Biological industries according to the manufacturer's protocol. To prepare normal and mutated YFP-p62 fusion constructs, we amplified the

control and mutated *nup62* cDNA using the following PCR primers: forward (incorporating the *XhoI* restriction site in the YFP gene): 5'-GCCTCGAGCCATGAGCGGGTTTA-ATTTTGGAG-3'; reverse (incorporating the *XbaI* restriction site downstream to the stop codon of the YFP gene): 5'-GCTCTAGAGTCGCTCAGTCAAAGGTGATCCGG-3'. The amplified cDNA of both normal and mutant *nup62* were ligated using T4 ligase (Promega, Madison, WI) to the YFP-plasmid digested with the *XhoI* and *XbaI* restriction enzymes.

TRANSFECTION AND IMMUNOFLUORESCENCE ANALYSIS. Human osteosarcoma cell line U2OS was cultured in Dulbecco's modified Eagle medium (DMEM; Gibco BRL, Life Technologies, Paisley, United Kingdom) supplemented with 10% fetal calf serum, 2mM glutamine, 100mg/ml streptomycin, and 100U/ml penicillin (Gibco BRL), at 37°C in a humidified incubator with 5% CO₂. U2OS cells were plated 24 hours before transfection at 2 × 10⁵ cells/well in a 6-well plate on coverslips and transfected transiently with YFP-p62 or YFP-mutant p62. Transfections were performed using the Jet PEI transfection reagent (Polyplus-Transfection, Illkirch, France). DNA amounts were kept constant by adding vector DNA (pCDNA3) when required. Twenty-four hours after transfection, the cells were fixed with ice-cold 4% paraformaldehyde for 30 minutes, then washed 3 times with TBS containing 0.1% Tween 20. The immunofluorescence procedure was performed using mouse monoclonal anti-p62 antibody as described earlier. Cells were analyzed using a 410 Zeiss confocal laser scan microscope (Zeiss, Oberkochen, Germany). The Zeiss LSM 410 is equipped with an ultraviolet laser (Coherent Inc. Lazer Group, Santa Clara, CA) and with a 25mW krypton-argon laser and a 10mW helium-neon laser (488, 543, and 633 maximum lines). A 63× numeric aperture/1.2 C Aplanachromat water-immersion lens (Axiocvert 135M; Zeiss) was used for all imaging. Series of 10 to 15 optical sections 2μm apart were obtained.

Bioinformatics Methods

Gene and protein descriptions were performed using UCSC and Ensembl genome browsers (assembly of May 2004) and bioinformatics servers. The best nine vertebrate (from fish to human) sequence homologues to human p62 protein were

collected using BLink ("BLAST Link"). Comparative sequence analysis (multiple sequence analysis [MSA]) was conducted by ClustalW with a Java viewer, as Higgins and colleagues¹⁵ and Clamp and coworkers¹⁶ described. ConSeq server was used to validate sequence conservation and predict functionality.¹⁷ The SIFT server sorts intolerant from tolerant amino acid substitutions and predicts phenotypic variations, as Ng and Henikoff¹⁸ described.

Results

Linkage Analysis

To refine the boundaries of the candidate region as defined by the markers D19S596 and D19S867 in a previous study,¹³ we searched publicly available sequence databases (UCSC Genome Browser, GDB) to identify six additional microsatellite markers and one single nucleotide polymorphism, which were used to genotype all the family members in the two critical pedigrees (Fig 1). Loss of homozygosity in Family 1 (Individuals II-2 and II-3) defined the centromeric border of the candidate region distally to the single nucleotide polymorphism rs8101959 in the gene *AP2A1* (see Fig 1). A recombination event was observed in Family 2, Individual II-4, defining the telomeric border of the candidate region and placing the disease-causing gene proximal to the polymorphic marker D19S867 (see Fig 1). Informative recombinations and the presence of a common haplotype indicated a minimal candidate interval of 230kb between markers rs8101959 and D19S867 (see Fig 1). The minimal candidate region contains 13 candidate genes (Fig 2A).

Mutation Analysis

Sequencing of the *nup62* gene in the minimal region of linkage showed a missense mutation (A→C), located 1,172bp downstream from the ATG translation initiation codon found in exon 3 (according to "Recommendations for the description of DNA sequence variants"; Ensembl genome browser; see Fig 2B). The

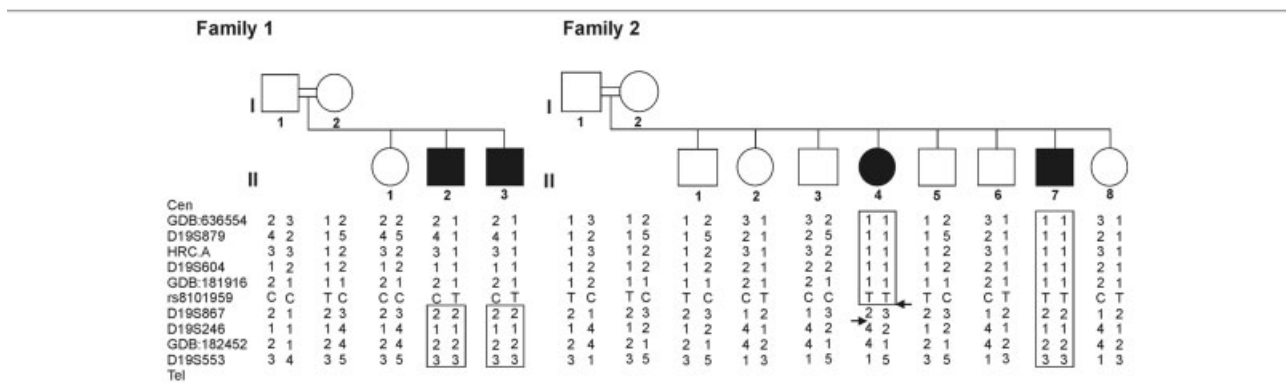


Fig 1. Fine mapping of the candidate region. The genotypes of two critical pedigrees with infantile bilateral striatal necrosis (IBSN). Black symbols in the pedigree represent affected individuals. Boxed regions indicate the homozygous regions in each affected individual. The polymorphic markers are shown on the left. Arrows indicate informative recombinations.

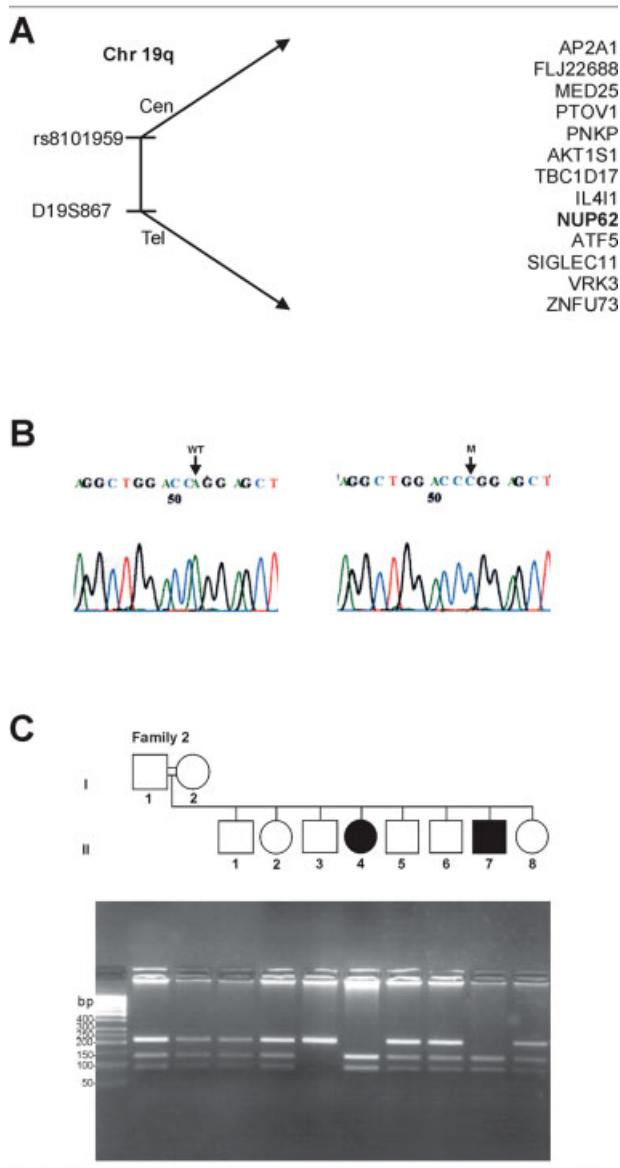


Fig 2. Candidate genes and mutation analysis of *nup62*. (A) Minimal candidate interval on chromosome 19, showing the genes in this region. (B) Sequence chromatogram from a wild-type (WT) and disease (M) genotype on genomic DNA. (C) Segregation of the mutation in *nup62* in the families as assayed by polymerase chain reaction (PCR) amplification of the genomic DNA and restriction by *NciI*. PCR product representing the WT allele is uncut.

mutation causes a change from glutamine to proline at the 391 residue (Q391P) in exon 3 of the *nup62* gene. In each pedigree analyzed, the *nup62* mutation segregated with the disease: Affected patients displayed homozygous mutations, whereas parents who were clinically normal displayed heterozygosity for a normal and a disease allele, consistent with recessive inheritance (see Fig 2C). The mutation was not observed in 620 chromosomes from unrelated control subjects of Jewish and Arab origin as determined by restriction enzyme

assay. However, this mutation has a frequency of 0.04 (12 heterozygotes in 280 chromosomes) in ethnically matched (Bedouin) control subjects living in the same village as the original family and the neighboring villages. All the heterozygous individuals also carried alleles corresponding to the alleles present in the disease-related haplotype in the several polymorphic markers adjacent to the mutation, indicating the same origin of the mutated allele.

All the other genes in the candidate region, including *AP2A1*, *MED25*, *PTOV1*, *PNKP*, *AKT1S1*, *TBC1D17*, *IL4I1*, *ATF5*, *SIGLECK11*, *VRK3*, the first two exons of *ZNF473*, and messenger RNA *GLARSEE*, were sequenced, and no pathogenic sequence changes were found.

Identification of the New Families and Prenatal Diagnosis

Two additional families bearing the same family name, including 2 affected and 11 unaffected individuals, were identified while this study was ongoing. The affected individuals were homozygous for the *nup62* mutation.

Five prenatal diagnoses were performed in three at-risk families. Two affected fetuses were found to be homozygous for the *nup62* mutation in two subsequent pregnancies in the same family. The first pregnancy was terminated, but the family decided to continue the second pregnancy, and the child started to show clinical signs of the disease at the age of 8 months. In the other families, the fetuses were found to be unaffected, and three healthy children were born, all of whom are currently developing normally.

Western Blot

We examined p62 expression by testing the proteins extracted from the lymphoblastoid cell line from each of the patients and control subjects by Western blot analysis. No reduction in the level of the mutated protein in the patients' cell lines was observed compared with the control subjects (Fig 3A).

Immunofluorescence and Transfection

We examined the effect of the mutation on the localization of the p62 protein in the nuclear membrane by immunofluorescent staining of control subject and patient lymphoblastoids. No differences were observed between the patient and control lymphoblastoid cells (see Fig 3B). In the transfected U2OS cells overexpressing normal and mutant YFP-p62 fusion protein, observation of the fluorescent signal showed diverse patterns of expression, including: (1) staining of the nuclear envelope with a fine punctuate pattern consistent with pore binding, (2) phase-dense cytoplasmic aggregates, and (3) diffuse cytoplasmic staining. These three staining patterns were in agreement with the pre-

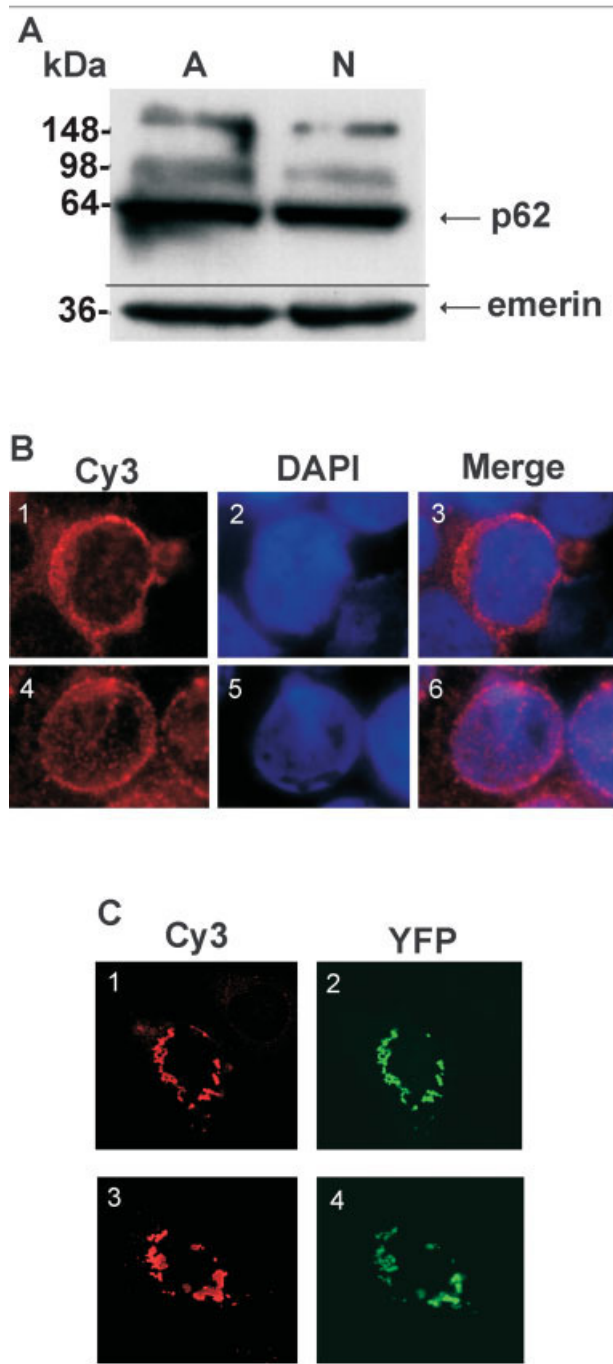


Fig 3. p62 protein analysis. (A) Western blot analysis of p62 in the lymphoblasts of affected (A) and normal (N) individuals. (B) Immunofluorescent staining of lymphoblastoid cells with p62 antibody from the affected (1–3) and normal (4–6) individuals. Cells were stained with primary p62 antibody followed by secondary Cy3-conjugated antibody (red). Nuclei were stained with 4',6'-diaminidino-2-phenylindole-2 hydrochloride (DAPI; blue). Merged images were created. (C) Confocal images of U2OS cells after transfection with mutated YFP-p62 and normal YFP-p62 constructs. Abnormal (1, 2) and normal (3, 4) cells were stained with primary p62 antibody followed by secondary Cy3-conjugated antibody (red). YFP-p62 construct fluorescence analysis was performed (green).

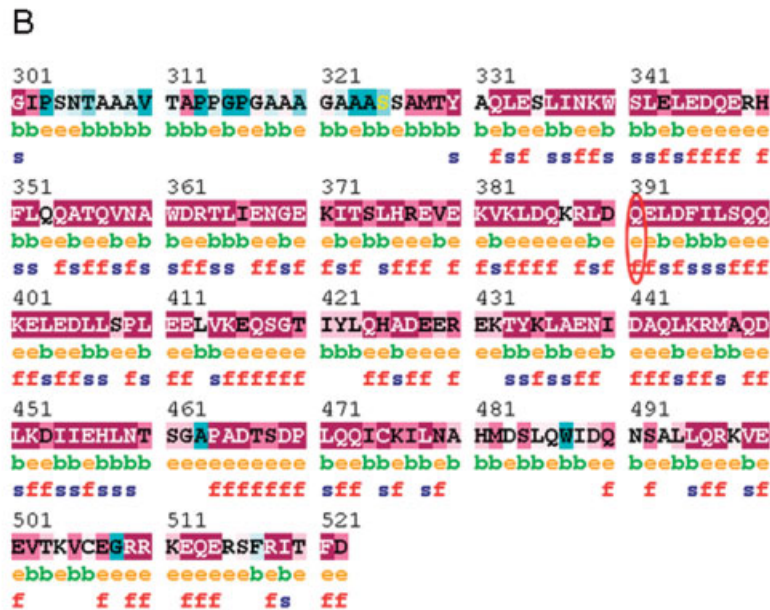
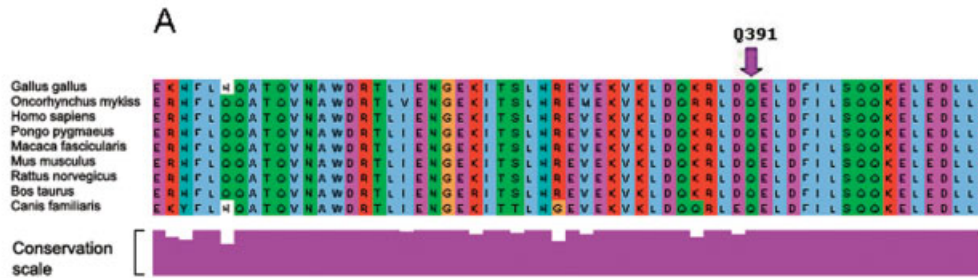
vious rat p62 expression studies.¹⁹ No differences between the normal and the mutated fusion protein signal were observed (see Fig 3C).

Gene and Protein Description Using Bioinformatics Tools

Nup62 gene (RefSeq constructed genomic contigs: NT_011109.15 and NT_086906.1) covers 22,705bp of genomic DNA. The *nup62* gene consists of a single promoter with a CpG island and three transcribed exons. The second exon is prone to alternative splicing.²⁰ The protein encoded by *nup62*, nuclear pore glycoprotein p62, is expressed ubiquitously in various tissues (see the GeneCards database).²⁰ All transcript variants encode a protein of 522 residues (National Center for Biotechnology Information: NP_036478; UniProt/Swiss-Prot: P37198; 53269 Da [GeneCards]). *Nup62* is embedded in introns 8 to 9 of the *IL4I1* gene (Ensembl OTTHUMG00000070945). Wiemann and colleagues²⁰ recently showed that the *IL4I1* gene is specifically transcribed from the apparent promoter of the upstream *nup62* gene in testis (Sertoli cells) and in the brain (eg, Purkinje cells); the first two exons of *nup62* are also contained in this novel *IL4I1* variant. However, because the first two exons are noncoding and the protein is encoded exclusively by the terminal third exon, we do not expect the mutation to affect the function of the protein encoded by this transcript. A single conserved domain Nsp1_C (Nsp1-like, C terminus) has been identified in the Pfam and InterPro databases (PF05064; residues 307–429; IPR007758; residues 310–432, respectively).

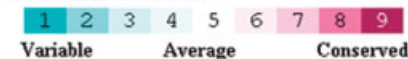
Multiple Sequence Analysis, ConSeq, and SIFT Results

Multiple alignment (MSA) was performed using nine protein sequence homologues of p62, including vertebrates from fish to human. MSA of amino acids 348 to 408 is shown in Figure 4A. An especially conserved region was found to be present at the C-terminal region of the protein, harboring the Nsp1-like C-terminal domain, which includes the Q391 residue of the human protein. Examination of amino acid conservation in the Pfam database also showed distant relatives of the family, including the yeast protein (*Saccharomyces cerevisiae*; Baker's yeast), which was shown to be highly conserved for glutamine at this position. However, *Caenorhabditis elegans* and *Schizosaccharomyces pombe* showed variations of the glutamine residue to R (arginine) and D (aspartic acid), respectively. Both R and D, as well as Q, are known to be hydrophilic and polar amino acids, with relatively similar characteristics. In conclusion, the region harboring Q391 in the human protein is most conserved in evolution, from yeast to mammals, and therefore variation at this point is predicted to lead to a severe change in protein function.



Legend:

The conservation scale:



- e** - An exposed residue according to the neural-network algorithm.
- b** - A buried residue according to the neural-network algorithm.
- f** - A predicted functional residue (highly conserved and exposed).
- s** - A predicted structural residue (highly conserved and buried).
- █** - Insufficient data - the calculation for this site was performed on less than 10% of the sequences.

Fig 4. Multiple alignment and conservation analysis of human p62 with its orthologues. (A) Multiple sequence alignment was performed by ClustalW, using nine protein sequences of p62, including vertebrates from fish to human (Homo sapiens [human], NP_036478; Macaca fascicularis [crab-eating macaque] BAE01812; Pongo pygmaeus [orangutan], CAH91435; Rattus norvegicus [rat], NP_075586; Mus musculus [mouse], Q63850; Gallus gallus [chick], XP_420179; Oncorhynchus mykiss [trout], AA24403; Bos taurus [cow], XP_615109; Canis familiaris [dog], XP_852888). An especially conserved region was found between residues 330 and 459 (348–408 are shown). Q391 in human is marked with a purple arrow. Residue colors represent amino acid biochemical properties according to Zappo colors. Conservation scale is shown below the alignment (purple). (B) Sequence conservation analysis was performed using ConSeq server. Multiple sequence analysis (MSA) results (A; residues 301–521) served as input. Results show the region containing the conserved domain (Nsp1_C domain), including residue Q391 (circled with red), that was found to be in the most conserved region. Most conserved regions are marked with dark magenta, and variable regions are marked with green. Exposed (e) and functional (f) predicted regions can be seen.

ConSeq server was applied to further support this conservation notion, using the same sequences as described earlier in MSA. Nsp1-like C-terminal domain is shown (see Fig 4B). Again, the Q391 position in the

human protein was found to be the most conserved. In addition, this region was predicted to be an exposed and functional region of the protein, supporting the hypothesized importance of it.

SIFT is a sequence homology-based tool that sorts intolerant from tolerant amino acid substitutions and predicts whether an amino acid substitution in a protein will have a phenotypic effect.¹⁸ Predicted results for residue Q391 in the human protein showed that the only tolerated changes in this amino acid may be to E (glutamic acid) or R (arginine), both of which are hydrophilic-polar amino acids, whereas a change to any other amino acid is predicted not to be tolerated.

Discussion

*Evidence That a *nup62* Mutation Causes Infantile Bilateral Striatal Necrosis*

There is much evidence that supports the role of the mutation in *nup62* as the cause of IBSN. First, sequencing of all the other genes in the candidate region showed no pathogenic mutations. Second, the Q391P mutation was not found in 620 control chromosomes from ethnically unrelated individuals, and it was found only in the heterozygous state in 280 control chromosomes from members of the Bedouin population originating in the same geographic area as the original families. The presence of such heterozygous individuals was expected because of the high frequency of carriers within this Bedouin population. Third, the Q391P mutation produces a substitution that results in a change from a polar, hydrophilic residue (acquired by the amide group) to a nonpolar, neutral residue. Glutamine plays an important structural role inside proteins by providing hydrogen bonding. Proline markedly influences protein architecture because its ring structure makes it more conformationally restricted, with a strong influence on protein folding, than all the other amino acids.²¹ Fourth, comparisons of p62 protein sequences from diverse species indicate that glutamine at position 391 is highly conserved. The region of Nsp1-like C terminus (amino acids 307–429) is almost completely identical in human, mouse, and rat, and mostly similar in all vertebrates (see Figs 4A, B). In addition, it is homologous to the essential yeast NSP1 carboxy-terminal domain, and therefore is presumably highly important in determining p62 function. Fifth, four patients in two new families identified during this study were found to be homozygous for the same *nup62* mutation.

The Disease-Causing Mechanism Does Not Involve Abnormal p62 Targeting or Anchoring to the Nuclear Pore Complex

The protein encoded by *nup62* belongs to the class of nucleoporins and is an essential part of the nuclear pore complex (NPC).^{22,23} The NPC is a massive structure that extends across the nuclear envelope, forming a gateway that regulates the flow of messenger RNA and proteins between the nucleus and the cyto-

plasm.^{24–26} The p62 protein encoded by *nup62* is a member of the phenylalanine-glycine (FG) repeats-containing nucleoporins.²⁷ This protein associates with the importin α/β complex, which is involved in the import of proteins containing nuclear localization signals.²⁸ The p62 protein appears to exist as a tight complex with at least two other proteins, p58 and p54.^{22,29} Rat p62 protein concentrates at the spindle poles during mitosis and in telophase is found in the region of condensed chromatin.¹⁹ Its N terminus is believed to be involved in nucleocytoplasmic transport, whereas the C-terminal end, which shows a hydrophobic heptad repeat organization similar to that found in lamins and other intermediate filament proteins, contains a coiled-coil structure aiding in protein–protein interactions and may function in anchorage of the protein in the pore complex.³⁰ Moreover, it was shown that the yeast Nsp1p coil 2 region, which is homologous to the region containing the mutation in our patients, has a role in both nuclear import and messenger RNA export, most likely because this region organizes two different heterodimeric subcomplexes, Nsp1p-Nup57p-Nup49p-Nic96p and Nsp1p-Nup82p-Nup159p, respectively.³¹ Normal immunostaining of the overexpressed YFP-p62 mutated protein in the U2OS cell line points to that p62 in our patients is still normally targeted and anchored to the NPC.

Nucleoporins and Mendelian Human Diseases

Only one gene encoding a protein localizing to a NPC that causes human mendelian disease has been described previously. Mutations in the WD repeat nucleoporin called ALADIN cause Allgrove's (triple A) syndrome.³² Triple A syndrome is characterized by adrenal insufficiency, abnormal development of the autonomic nervous system causing achalasia of the esophagus and alacrima, and late-onset progressive neurological symptoms (including cerebellar ataxia, peripheral neuropathy, and mild dementia). Characterization of mutant ALADIN proteins from triple A syndrome patients demonstrated defective NPC targeting.³³ Mutant protein failed to localize to NPCs and was found predominantly in the cytoplasm. The mutation in *nup62* described in this study is the second example of a NPC protein causing mendelian disease in humans. Both diseases share central nervous system involvement. The Q391P mutation does not affect localization of the mutant protein to NPCs, suggesting another, as yet unknown, biological cell type-specific mechanism or mechanisms that cause basal ganglia disease in our patients. Numerous possible models can be hypothesized, including delicate changes in the NPC structure or the abnormal transport pathway of a specific, as yet unknown, protein in neuronal cells in basal ganglia. Alternatively, the mutation might affect chromatin organization in the specific cell type in the central nervous system. The identification of proteins

that can no longer interrelate properly with the mutant protein would be a future goal.

Electronic Database Information

Accession numbers and URLs for data presented herein are as follows:

Online Mendelian Inheritance in Man (OMIM):
<http://www.ncbi.nlm.nih.gov/Omim>

Primer3: http://frodo.wi.mit.edu/cgi-bin/primer3/primer3_www.cgi

UCSC Genome Browser: <http://genome.cse.ucsc.edu>

Ensembl Genome Browser: <http://www.ensembl.org>

BLink: <http://www.ncbi.nlm.nih.gov/entrez/query.fcgi?db=Protein>

GeneBank; BLAST: <http://www.ncbi.nlm.nih.gov/BLAST>

Entrez protein search: <http://www.ncbi.nlm.nih.gov/Entrez>

ClustalW (multiple sequence alignment with a Java viewer): <http://www.hongyu.org/software/clustal.html>

ConSeq: <http://conseq.bioinfo.tau.ac.il>

SIFT: http://blocks.fhcrc.org/sift/SIFT_seq_submit2.html

Genome Database: <http://www.gdb.org>

Human Genome Variant Society: Recommendations for the description of DNA sequence variants:
<http://www.hgvs.org/mutnomen/recs-DNA.html>

RefSeq: <http://www.ncbi.nlm.nih.gov/RefSeq>

GO browser: <http://www.ebi.ac.uk/ego>

GeneCards: <http://www.genecards.org/cgi-bin/carddisp?NUP62>

UniProt/Swiss-Prot: <http://www.ebi.ac.uk/swissprot>

Pfam: <http://www.sanger.ac.uk/Software/Pfam>

Interpro: <http://www.ebi.ac.uk/InterProScan>

This study was funded by the Yeshaya Horovitz Grant for Neurogenetics Research. Part of this work was performed in partial fulfillment of the requirements of the PhD program at the Sackler School of Medicine (Tel Aviv University, L.M.).

We are grateful to the families who participated in this study. We also thank Dr G. Halpern for her help with editing the manuscript, I. Lis for preparing the figures, and Drs A. Harel and D. J. Forbes for providing polyclonal p62 antibody. We thank Dr D. Gurevitch for establishing the lymphoblastoid cell line and L. Mittelman for his assistance with confocal microscopy.

References

1. Friede RL. Developmental neuropathology. Vienna: Springer-Verlag, 1974:88–89.
2. Leuzzi V, Favata I, Seri S. Bilateral striatal lesions. *Dev Med Child Neurol* 1988;30:252–257.
3. Paterson D, Carmichael EA. A form of familial cerebral degeneration chiefly affecting the lenticular nucleus. *Brain* 1924;47:207–231.

4. Bargeton-Farkas E, Cochard AM, Brissaud HE, et al. Familial infantile encephalopathy with symmetric bilateral necrosis of the corpus striatum. *J Neurol Sci* 1964;11:429–445.
5. Miyoshi K, Matsuoka T, Mizushima S. Familial holotopistic striatal necrosis. *Acta Neuropathol (Berl)* 1969;13:240–249.
6. Roessmann U, Schwartz JF. Familial striatal degeneration. *Arch Neurol* 1973;29:314–317.
7. Mito T, Tanaka T, Becker LE, et al. Infantile bilateral striatal necrosis: clinicopathological classification. *Arch Neurol* 1986;43:677–680.
8. Holtzman D, Hedley-Whyte ET. CPC. Case records of the Massachusetts General Hospital. Case 30-1992. Progressive neurodegenerative disease in a young boy. *N Engl J Med* 1992;327:261–268.
9. Gieron MA, Gilbert-Barnes E, Vonsattel JP, Korthals JK. Infantile progressive striatohalamic degeneration in two siblings: a new syndrome. *Pediatr Neurol* 1995;12:260–263.
10. De Meirleir L, Seneca S, Lissens W, et al. Bilateral striatal necrosis with a novel point mutation in the mitochondrial ATPase 6 gene. *Pediatr Neurol* 1995;13:242–246.
11. Thyagarajan D, Shanske S, Vazquez-Memije M, et al. A novel mitochondrial ATPase 6 point mutation in familial bilateral striatal necrosis. *Ann Neurol* 1995;38:468–472.
12. Straussberg R, Shorer Z, Weitz R, et al. Familial infantile bilateral striatal necrosis: clinical features and response to biotin treatment. *Neurology* 2002;59:983–989.
13. Basel-Vanagaite L, Straussberg R, Ovadia H, et al. Infantile bilateral striatal necrosis maps to chromosome 19q. *Neurology* 2004;62:87–90.
14. Sambrook J, Fritsch E, Maniatis T. Molecular cloning: a laboratory manual. 2nd ed. New York: Cold Spring Harbor Laboratory Press, 1989.
15. Higgins D, Thompson J, Gibson T, et al. CLUSTAL W: improving the sensitivity of progressive multiple sequence alignment through sequence weighting, position-specific gap penalties and weight matrix choice. *Nucleic Acids Res* 1994;22:4673–4680.
16. Clamp M, Cuff J, Searle SM, Barton GJ. The Jalview Java Alignment Editor. *Bioinformatics* 2004;20:426–427.
17. Berezin C, Glaser F, Rosenberg J, et al. ConSeq: the identification of functionally and structurally important residues in protein sequences. *Bioinformatics* 2004;20:1322–1324.
18. Ng PC, Henikoff S. Accounting for human polymorphisms predicted to affect protein function. *Genome Res* 2002;12:436–446.
19. Starr CM, D'Onofrio M, Park MK, Hanover JA. Primary sequence and heterologous expression of nuclear pore glycoprotein p62. *J Cell Biol* 1990;110:1861–1871.
20. Wiemann S, Kolb-Kokocinski A, Poustka A. Alternative pre-mRNA processing regulates cell-type specific expression of the *IL4I1* and *NUP62* genes. *BMC Biol* 2005;3:16.
21. Berg JM, Tymoczko JL, Stryer L. Biochemistry. 5th ed. New York: W.H. Freeman, 2002.
22. Finlay DR, Meier E, Bradley P, et al. A complex of nuclear pore proteins required for pore function. *J Cell Biol* 1991;114:169–183.
23. Hetzer MW, Walther TC, Mattaj IW. Pushing the envelope: structure, function, and dynamics of the nuclear periphery. *Annu Rev Cell Dev Biol* 2005;21:347–380.
24. Dargemont C, Schmidt-Zachmann MS, Kuhn LC. Direct interaction of nucleoporin p62 with mRNA during its export from the nucleus. *J Cell Sci* 1995;108:257–263.
25. Allen TD, Cronshaw JM, Bagley S, et al. The nuclear pore complex: mediator of translocation between nucleus and cytoplasm. *J Cell Sci* 2000;113:1651–1659.

26. Cronshaw JM, Krutchinsky AN, Zhang W, et al. Proteomic analysis of the mammalian nuclear pore complex. *J Cell Biol* 2002;158:915–927.
27. Ryan KJ, Wentz SR. The nuclear pore complex: a protein machine bridging the nucleus and cytoplasm. *Curr Opin Cell Biol* 2000;12:361–371.
28. Percipalle P, Clarkson WD, Kent HM, et al. Molecular interactions between the importin alpha/beta heterodimer and proteins involved in vertebrate nuclear protein import. *J Mol Biol* 1997;266:722–732.
29. Kita K, Omata S, Horigome T. Purification and characterization of a nuclear pore glycoprotein complex containing p62. *J Biochem* 1993;113:377–382.
30. Carmo-Fonseca M, Kern H, Hurt EC. Human nucleoporin p62 and the essential yeast nuclear pore protein NSP1 show sequence homology and a similar domain organization. *Eur J Cell Biol* 1991;55:17–30.
31. Bailer SM, Balduf C, Hurt E. The Nsp1p carboxy-terminal domain is organized into functionally distinct coiled-coil regions required for assembly of nucleoporin subcomplexes and nucleocytoplasmic transport. *Mol Cell Biol* 2001;21:7944–7955.
32. Tullio-Pelet A, Salomon R, Hadj-Rabia S, et al. Mutant WD-repeat protein in triple-A syndrome. *Nat Genet* 2000;26:332–335.
33. Cronshaw JM, Matunis MJ. The nuclear pore complex protein ALADIN is mislocalized in triple A syndrome. *Proc Natl Acad Sci U S A* 2003;100:5823–5827.